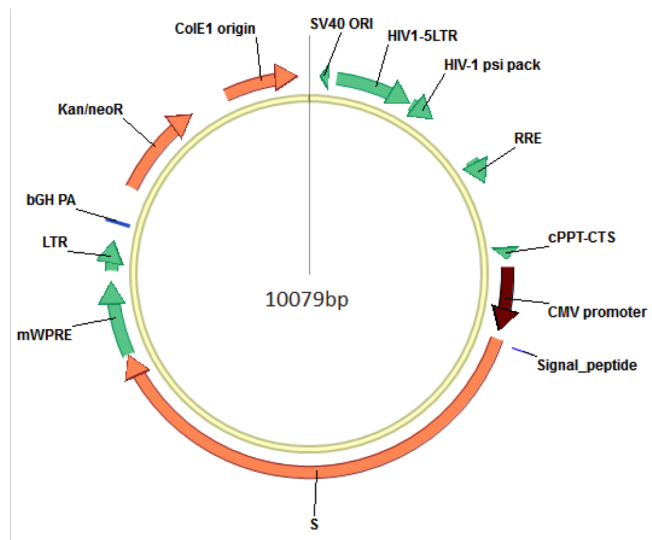


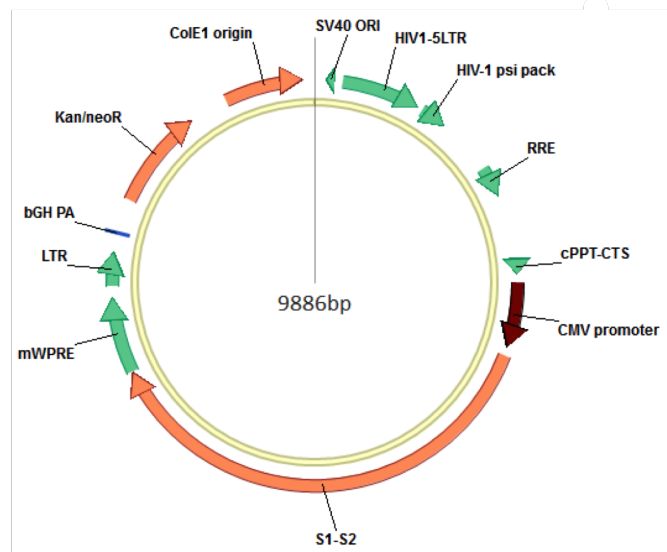
## **Supplemental Information**

### **Intranasal vaccination with a lentiviral vector protects against SARS-CoV-2 in preclinical animal models**

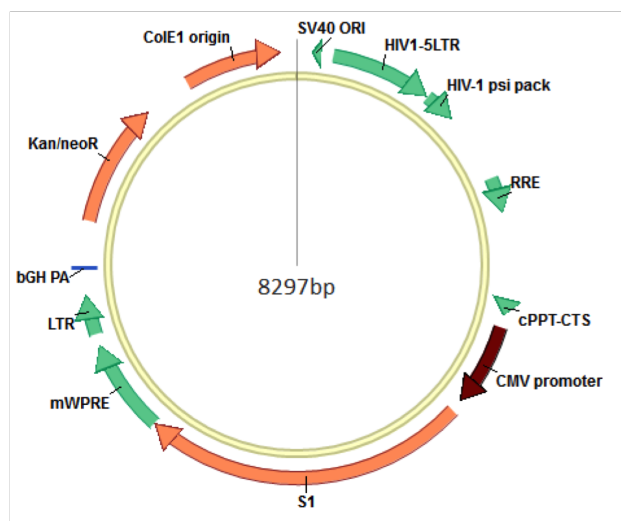
**Min-Wen Ku, Maryline Bourguin, Pierre Authié, Jodie Lopez, Kirill Nemirov, Fanny Moncoq, Amandine Noirat, Benjamin Vesin, Fabien Nevo, Catherine Blanc, Philippe Souque, Houda Tabbal, Emeline Simon, David Hardy, Marine Le Dudal, Françoise Guinet, Laurence Fiette, Hugo Mouquet, François Anna, Annette Martin, Nicolas Escriou, Laleh Majlessi, and Pierre Charneau**



**pFlap-CMV-S<sub>FL</sub>-WPREm**



**pFlap-CMV-S1-S2-WPREm**

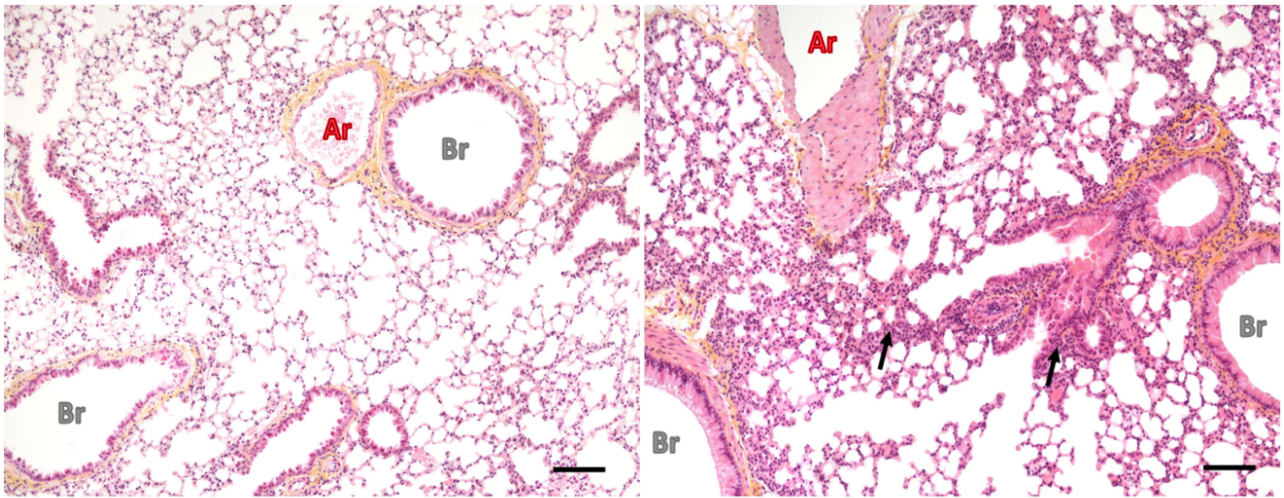


**pFlap-CMV-S1-WPREm**

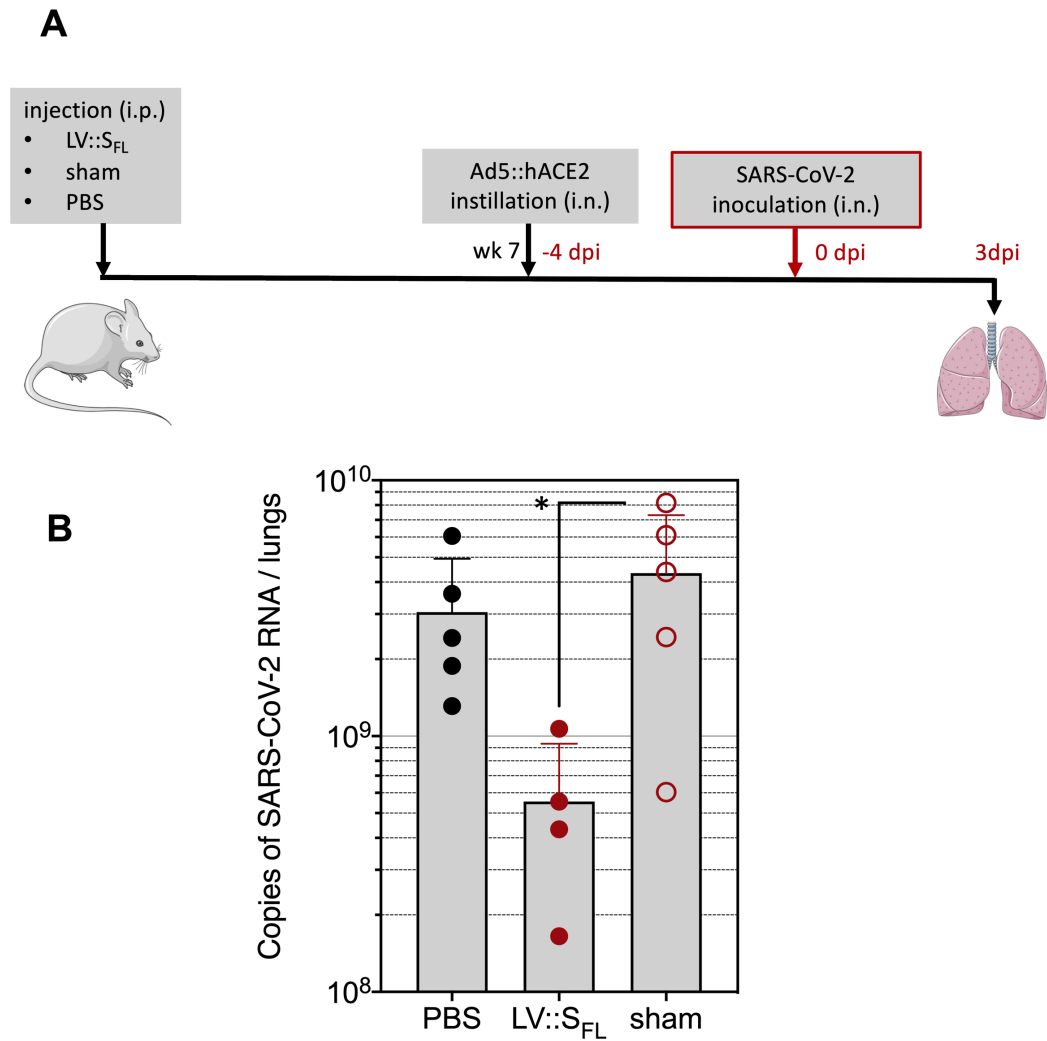
**Figure S1. Maps of plasmids used for production of LV encoding S<sub>FL</sub>, S1-S2 or S1 antigens, related to Figure 1 and STAR Methods.**

i.n. PBS  
i.n. SARS-CoV-2

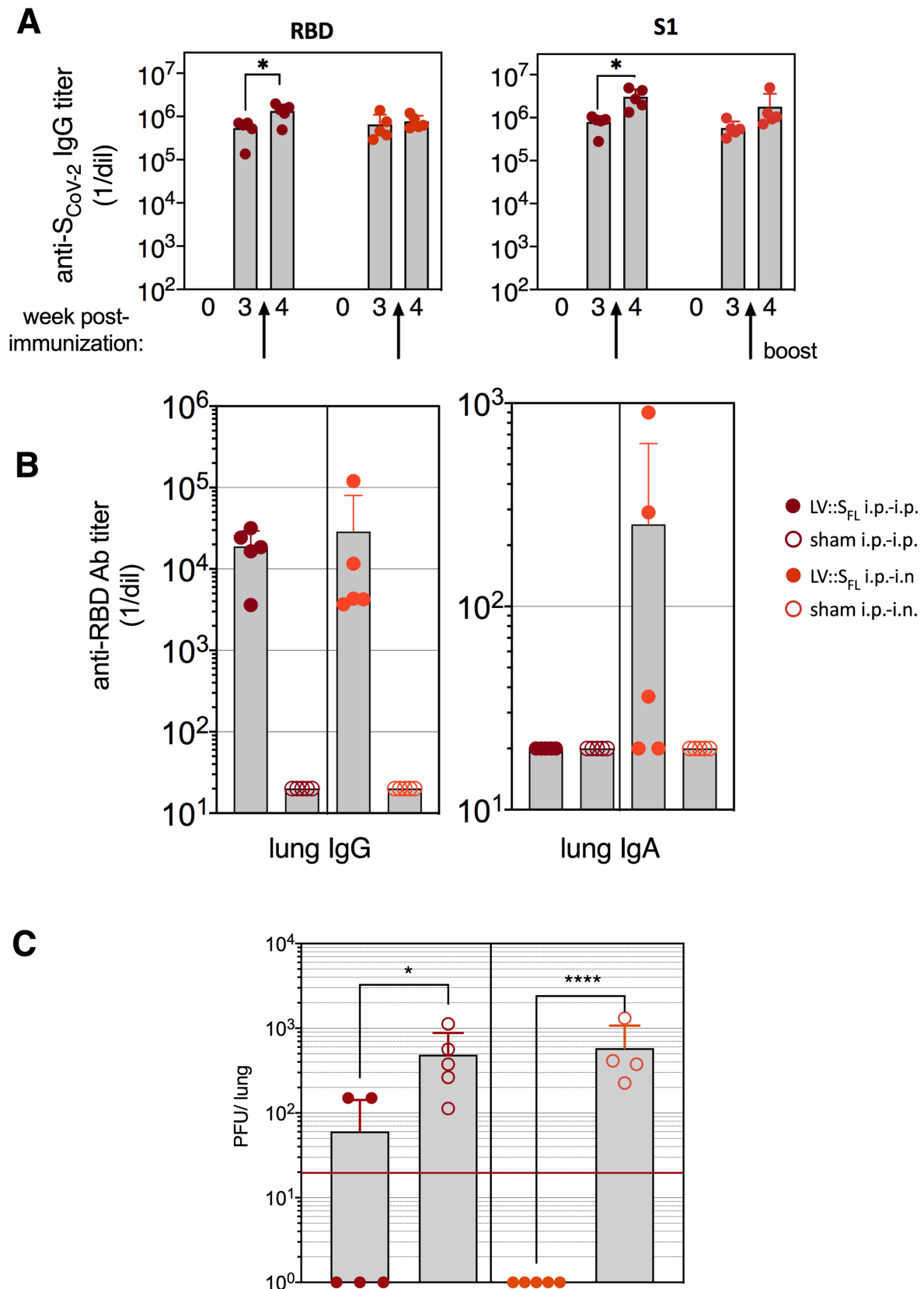
i.n. Ad5::hACE-2  
i.n. SARS-CoV-2



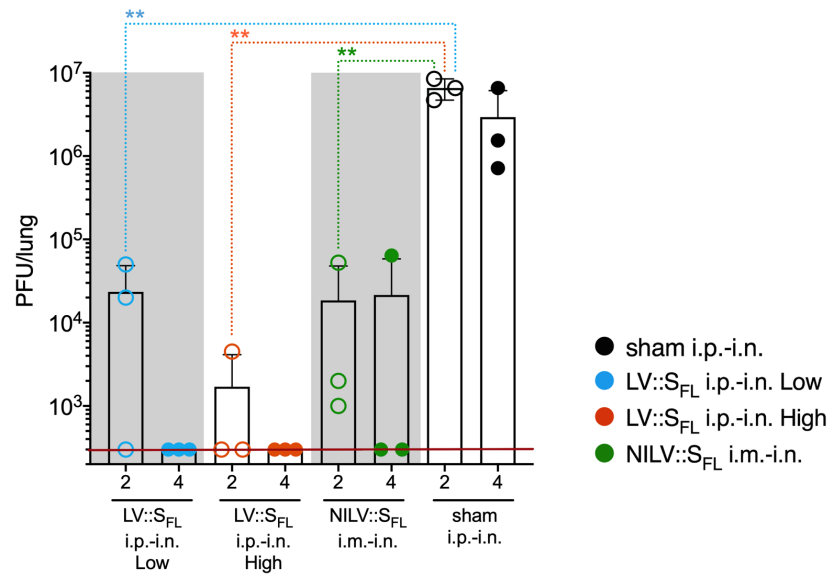
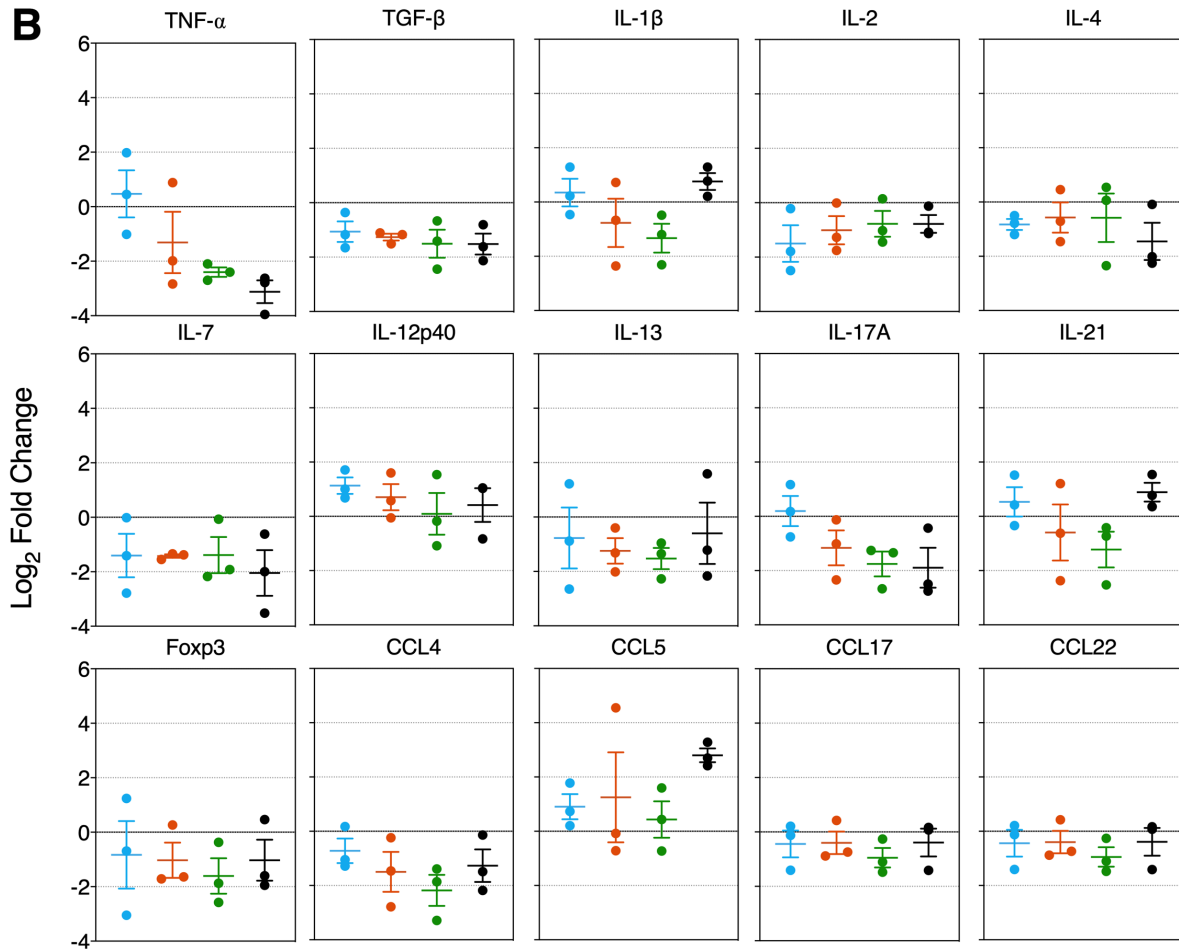
**Figure S2. Lung histology in mice pretreated with Ad5::hACE2 and inoculated with SARS-CoV-2 related to Figure 3.** Histological analysis in C57BL/6 mice, pretreated with PBS or Ad5::hACE2, followed by i.n. inoculation of  $1 \times 10^5$  TCID<sub>50</sub> of SARS-CoV-2. Analysis was performed at 3 dpi. Lung, HE&S stain, Original magnification: x10, scale bar: 100  $\mu$ m. Br: Bronchi or bronchiole. Bv: Blood vessel. Arrow: Mononuclear inflammatory cell infiltration.



**Figure S3. Protective potential of systemic immunization with LV::S<sub>FL</sub> against SARS-CoV-2 in mice, related to Figure 4. (A)** Timeline of vaccination by a single i.p. injection of LV followed by Ad5::hACE2 pretreatment and i.n. SARS-CoV-2 challenge. **(B)** Lung viral loads in unvaccinated mice (PBS), LV::S<sub>FL</sub>- or sham-vaccinated mice, at 3 dpi. Statistical significance of the differences in the viral loads was evaluated by two tailed unpaired t test; \* =  $p < 0.0139$ .



**Figure S4. Serum or lung homogenate Ab responses against RBD or S1 and lung viral PFU, related to Figure 4.** (A) Titers of anti-S<sub>CoV-2</sub> IgG, able to bind to S1 or RBD fragments of S<sub>CoV-2</sub>, as quantitated by ELISA in the sera of C57BL/6 mice primed i.p. at week 0 and boosted i.p. or i.n. at week 3. \*  $p < 0.01$ ; two-way ANOVA followed by Sidak's multiple comparison test. NS, not significant. Neutralization capacity of these sera, indicated as EC<sub>50</sub> (right). (B) Titers of anti-S<sub>CoV-2</sub> IgG and IgA Abs, as determined in the clarified lung homogenates by ELISA using RBD in coating. (C) Lung viral infectious particles, quantified as PFU at 3 dpi. The red line indicates the detection limit of the PFU assay. Statistical significance of the differences in the viral loads was evaluated by two tailed unpaired t test; \* =  $p < 0.05$ , \*\*\*\* =  $p < 0.0001$ .

**A****B**

**Figure S5. Characteristics of golden hamsters vaccinated with LV::S<sub>FL</sub> and protected against SARS-CoV-2, related to Figure 6. (A)** Lung viral infectious particles in LV::S<sub>FL</sub>-vaccinated and protected hamsters versus unprotected sham-vaccinated individuals, quantified as PFU at 2 or 4 dpi. The red line indicates the detection limit. Statistical significance of the differences in the viral loads was evaluated by two tailed unpaired t test; \*\* =  $p < 0.01$ . **(B)** inflammation mediators in the lungs of LV::S<sub>FL</sub>- or sham-vaccinated and challenged hamsters. Relative  $\log_2$  fold changes in cytokines and chemokines mRNA expression in LV::S<sub>FL</sub>-vaccinated and protected hamsters versus unprotected sham-vaccinated individuals, as determined at 4 dpi by qRT-PCR in the total lung homogenates and normalized to the mean of untreated controls. Shown are the inflammatory mediators for which the differences between the LV::S<sub>FL</sub>- and sham-vaccinated hamsters were not statistically different, as evaluated by one-way ANOVA.

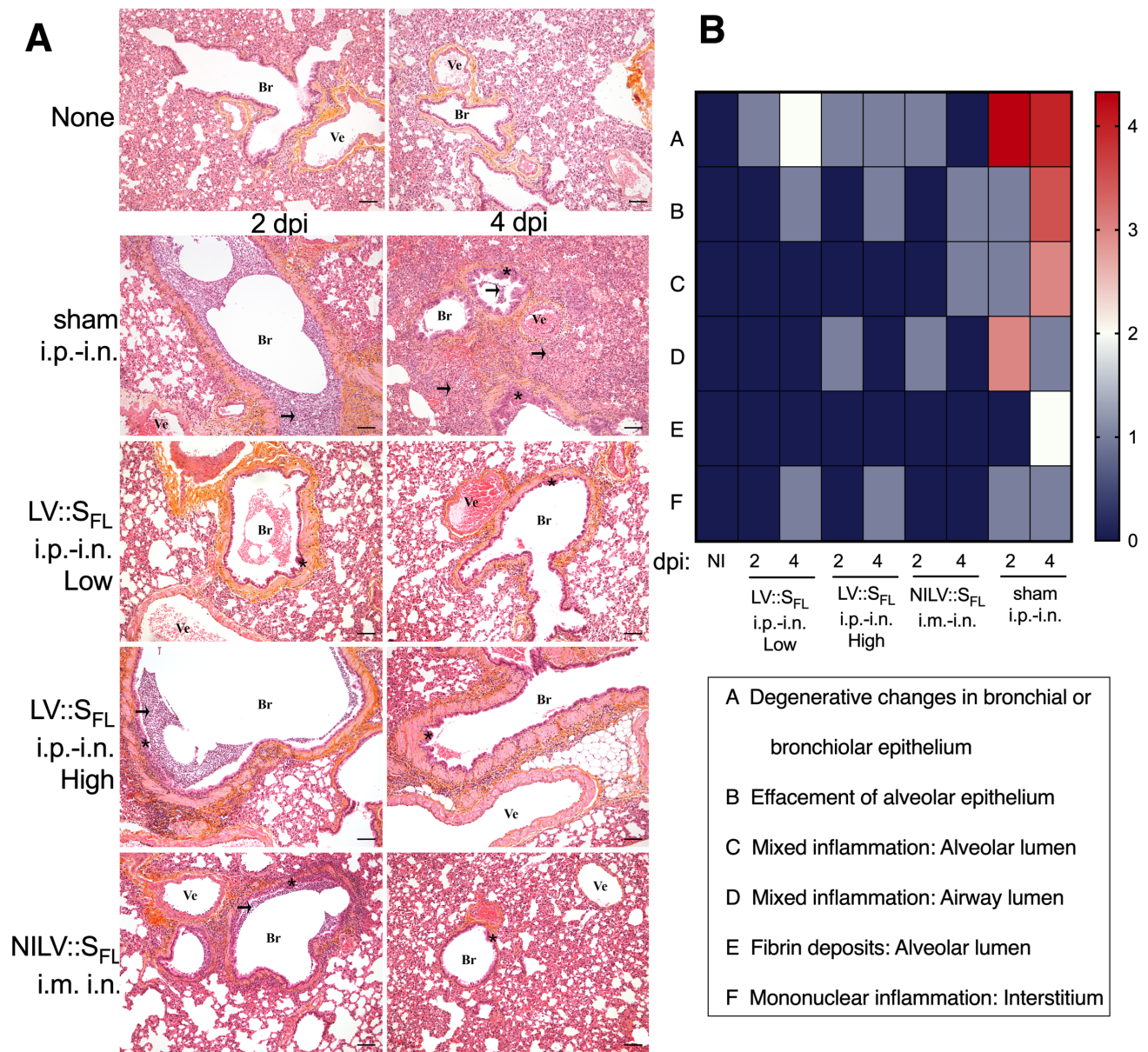


**Figure S6. LV::S<sub>FL</sub> vaccination reduces SARS-Co-2-mediated histopathology in golden hamsters, related to Figure 6.** Animals are those detailed in the Figure 6. **(A)** Histological analysis HE&S lung shown for 2 and 4 dpi. Original magnification: x10, scale bar: 100  $\mu$ m. Br: Bronchi or bronchiole. Bv: Blood vessel. Arrow: Mononuclear inflammatory cell infiltration. Star: Degenerative changes in the respiratory epithelium. **(B)** Heatmap recapitulating the average of histological scores, for each defined parameter and determined for individuals of the same groups at 2 or 4 dpi.

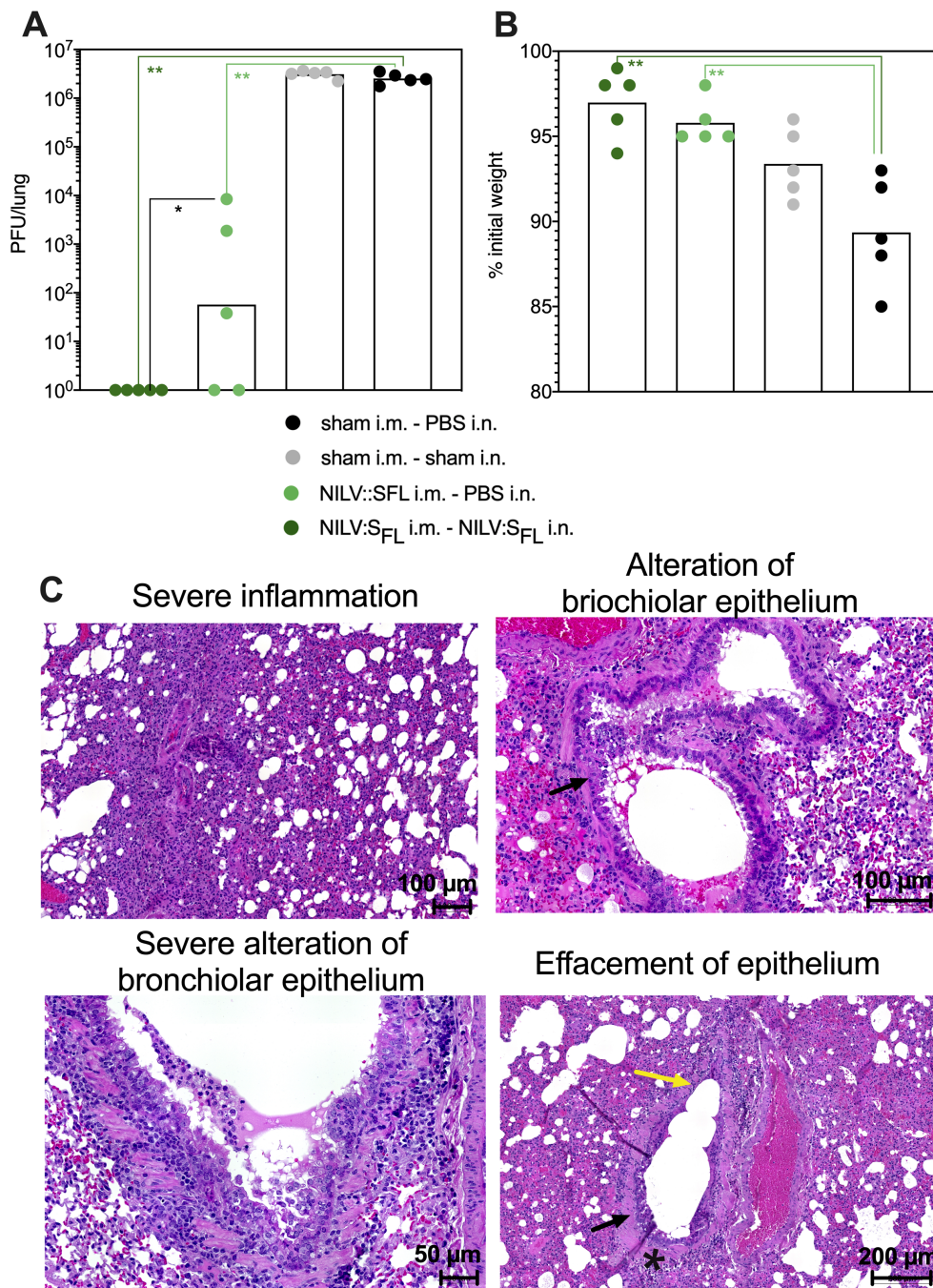


**Figure S7. Protective efficacy of NILV::S<sub>FL</sub> in a systemic prime and intranasal boost regimen in golden hamsters, related to Figure 7. (A) Lung viral loads and (B) weight loss at 4 dpi with SARS-CoV-2 in controls or NILV::S<sub>FL</sub>-vaccinated hamsters. Statistical significance of the differences in the viral loads was evaluated by two tailed unpaired t test; \*\* =  $p < 0.001$ , \* =  $p < 0.01$ . (C). Examples of histology lesions. The upper left panel depicts a severe parenchymal inflammation, characterized by an intense mononuclear cell infiltration, which still leaves patches of cell-free areas. In the upper right panel, the general organization of the bronchiolar epithelium is preserved and most nuclei against the basal membrane look normal, however, there is some degree of degenerative changes (arrows), and an aggregate of detached cells as well as red blood cells and fibrinous material partially fill the bronchiolar lumen. The lower left panel depicts a more advanced stage of bronchiolar epithelium alteration; epithelial cells are swollen, contain apoptotic nuclei and slough off in the lumen in large numbers. The lamina propria is infiltrated and at places the separation between epithelium and muscle is obliterated. These destructive processes eventually lead to epithelium effacement, as in the example shown in the lower right panel; here, the bronchiole is identifiable by the peribronchiolar muscle (star) and by remnants of a pseudostratified epithelium (black arrow), which is no longer discernable in the upper part of the picture (yellow arrow).**

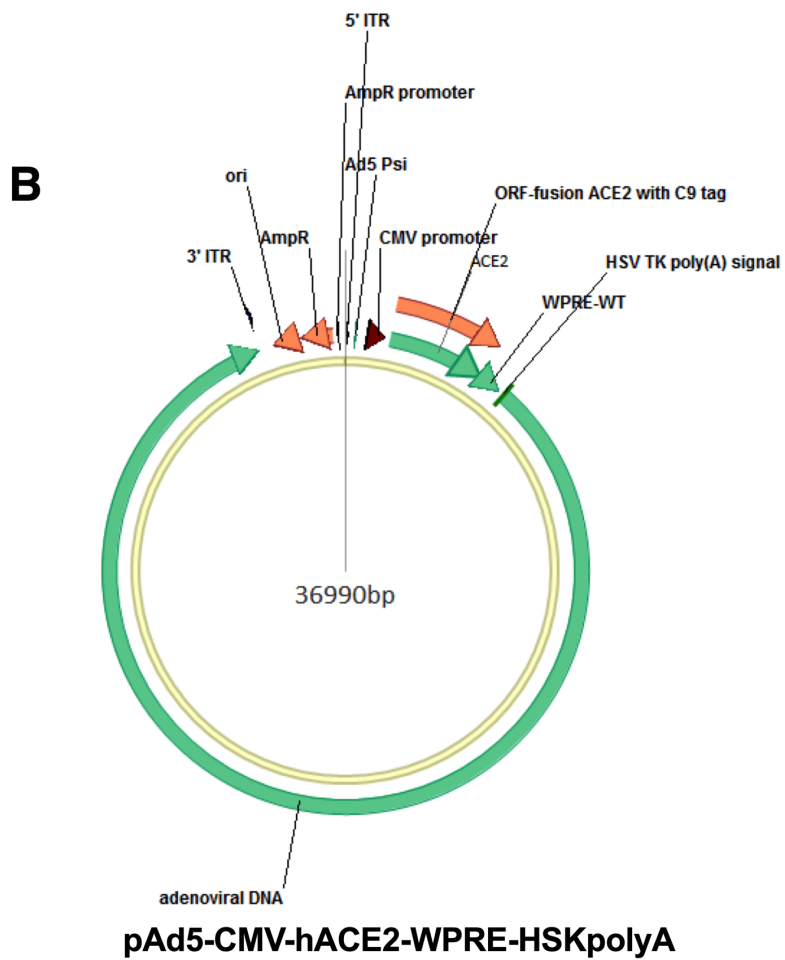
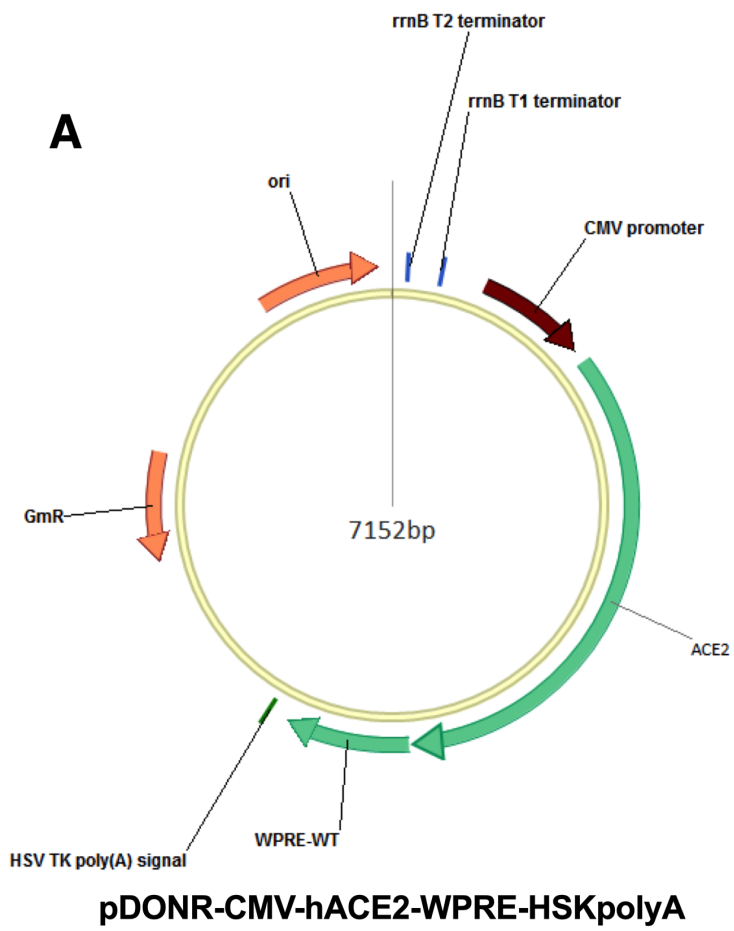


**Figure S8. Maps of plasmids used for production of Ad5 encoding hACE2 related to STAR Methods.**

Primer/Probe Name	DNA Sequences
“E-Sarbeco” Fw	5’-ACAGGTACGTTAATAGTTAATAGCGT-3’
“E-Sarbeco” Rv	5’-ATATTGCAGCAGTACGCACACA-3’
“E-Sarbeco” Probe	5’-FAM-ACACTAGCCATCCTTACTGCGCTTCG- BHQ-1-3’

**Table S1. Sequences of primers and probes for SARS-CoV-2 viral load determination related to STAR Methods.**

## Sequences

## Mouse Gene

$\beta$ -globin	F : 5'- ATGGGAAGCCGAACATACTG -3' R : 5'- CAGTCTCAGTGGGGGTGAAT -3'
GAPDH	F : 5'- TTCACCACCATGGAGAAGGC -3' R : 5'- GGCATGGACTGTGGTCATGA -3'
IFN $\alpha$	F : 5'- GGATGTGACCTTCCTCAGACTC -3' R : 5'- ACCTTCTCCTGCGGAATCCAA -3'
IFN $\gamma$	F : 5'- TCAAGTGGCATAGATGTGGAAGAA -3' R : 5'- TGGCTCTGCAGGATTTTCATG -3'
TNF $\alpha$	F : 5'- CATCTTCTCAA AATTCGAGTGACAA -3' R : 5'- TGGGAGTAGACAAGGTACAACCC -3'
TGF $\beta$	F : 5'- TGACGTC ACTGGAGTTGTACGG -3' R : 5'- GGTT CATGTCATGGATGGTGC -3'
IL1 $\beta$	F : 5'- TGGACCTTCCAGGATGAGGACA -3' R : 5'- GTTCATCTCGGAGCCTGTAGTG -3'
IL2	F : 5'- CCTGAGCAGGATGGAGAATTACA -3' R : 5'- TCCAGAACATGCCGCAGAG -3'
IL4	F : 5'- CGAGGTCACAGGAGAAGGGA -3' R : 5'- AAGCCCTACAGACGAGCTCACT -3'
IL5	F : 5'- GATGAGGCTTCCTGTCCCTACT -3' R : 5'- TGACAGGTTTTGGAATAGCATTTC -3'
IL6	F : 5'- CTGCAAGTGCATCATCGTTGTTT -3' R : 5'- TACCACTTCACAAGTCGGAGGC -3'
IL10	F : 5'- GGTTGCCAAGCCTTATCGGA -3' R : 5'- ACCTGCTCCACTGCCTTGCT -3'
IL12p40	F : 5'- GGAAGCACGGCAGCAGAATA -3' R : 5'- AACTTGAGGGAGAAGTAGGAATGG -3'
IL17A	F : 5'- GAAGCTCAGTGCCGCCA -3' R : 5'- TTCATGTGGTGGTCCAGCTTT -3'
IL18	F : 5'- GACAGCCTGTGTTTCGAGGATATG -3' R : 5'- TGTTCTTACAGGAGAGGGTAGAC -3'
IL33	F : 5'- CTACTGCATGAGACTCCGTTCTG -3' R : 5'- AGAATCCCGTGGATAGGCAGAG -3'
CCL2	F : 5'- AGGTCCTGTCATGCTTCTG -3' R : 5'- TCTGGACCCATTCCTTCTTG -3'
CCL3	F : 5'- CCTCTGTCACCTGCTCAACA -3' R : 5'- GATGAATTGGCGTGGAATCT -3'
CCL5	F : 5'- GTGCCACGTCAAGGAGTAT -3' R : 5'- GGAAGCGTATACAGGGTCA -3'
CXCL5	F : 5'- GCATTTCTGTTGCTGTTACGCTG -3' R : 5'- CCTCCTTCTGGTTTTTCAGTTTAGC -3'
CXCL9	F : 5'- AAAATTTTCATCACGCCCTTG -3' R : 5'- TCTCCAGCTTGGTGAGGTCT -3'
CXCL10	F : 5'- GGATGGCTGTCCTAGCTCTG -3' R : 5'- ATAACCCCTTGG GAAGATGG -3'

## Hamster gene

$\beta$ 2-Microglobulin	F : 5'- GGCTCACAGGGAGTTTGTAC -3' R : 5'- TGGGCTCCTTCAGAGTTATG -3'
RLP18	F : 5'- GTTTATGAGTCGCACTAACCG -3' R : 5'- TGTTCTCTCGGCCAGGAA -3'
IFN $\gamma$	F : 5'- TGTTGCTCTGCCTCACTCAGG -3' R : 5'- AAGACGAGGTCCCCTCCATTC -3'
TNF $\alpha$	F : 5'- TGAGCCATCGTGCCAATG -3'

TGFβ	R : 5'- AGCCCGTCTGCTGGTATCAC -3' F : 5'- GGCTACCACGCCAACTTCTG -3' R : 5'- GAGGGCAAGGAC CTTACTGTACTG -3'
IL1β	F : 5'- GGCTGATGCTCCCATTCTG -3' R : 5'- CACGAGGCATTTCTGTTGTTCA -3'
IL2	F : 5'- GTGCACCCACTTCAAGCTCTAA -3' R : 5'- AAGCTCCTGTAAAGTCCAGCAGTAAC -3'
IL4	F : 5'- ACAGAAAAAGGGACACCATGCA -3' R : 5'- GAAGCCCTGCAGATGAGGTCT -3'
IL6	F : 5'- AGACAAAGCCAGAGTCATT -3' R : 5'- TCGGTATGCTAAGGCACAG -3'
IL7	F : 5'- ATCAGCATCGATGAATTGGACAAA -3' R : 5'- CTTGCGAGCAGCACGATTTA -3'
IL10	F : 5'- GGTGCGCAAACCTTATCAGAAATG -3' R : 5'- TTCACCTGTTCCACAGCCTTG -3'
IL12p40	F : 5'- AATGCGAGGCAG CAAATTACTC -3' R : 5'- CTGCTCTTGACGTTGAACTTCAAG -3'
IL13	F : 5'- AAATGGCGGGTTCTGTGC -3' R : 5'- AATATCCTCTGGGTCTTGTAGATGG -3'
IL17A	F : 5'- GAGGGAAAGTTGGACCACCA -3' R : 5'- GACAATGGAGGAAACGCAGG -3'
IL21	F : 5'- GGACAGTGGCCATA AAACAAG -3' R : 5'- TTCAACACTGTCTATAAGATGACGAAGTC -3'
Foxp3	F : 5'- GGTCTTCGAGGAGCCAGAAGA -3' R : 5'- GCCTTGCCCTTCTCATCCA -3'
CCL2	F : 5'- CCGTAACTCCCCACTCACC -3' R : 5'- TGAGCTTGGTGATGAAAATCACAG -3'
CCL3	F : 5'- CTCTGAGCCAGGTGTCATTTTC -3' R : 5'- CCCAGGTTTCTTTGGGGTCA -3'
CCL4	F : 5'- GCTTGGTCACGTGGTCAGTG -3' R : 5'- GTGGTTGCGCTCCGT GTAG -3'
CCL5	F : 5'- ACTGCCTCGTGTTACATCA -3' R : 5'- TTCGGGTGACAAAAACGACT -3'
CCL17	F : 5'- GTGCTGCCTGGAGATCTTCA -3' R : 5'- TGGCATCCCTGGGACACT -3'
CCL22	F : 5'- TGGTGCCAA CGTGGAAGAC -3' R : 5'- GAAGAACTCCTTCACTACGCGC -3'
CXCL10	F : 5'- GCCATTCATCCACAGTTGACA -3' R : 5'- CATGGTGCTGACAGTGGAGTCT -3'

**Table S2. Sequences of primers used to quantitate cytokines and chemokines by qRT-PCR related to STAR Methods.**